3D printing MOFs-reinforced flame-retardant PA12 composites with customizable structures

Nannan Wang[a], Can Wei[a], Feng Wei[a], Fangdi Huang[a], Ding Chen[a,b]*, Chunze Yan[d], Yanqiu Zhu[a,c]*

[a] Key Laboratory of Disaster Prevention and Structural Safety of Ministry of Education, Guangxi Key Laboratory of Disaster Prevention and Engineering Safety, School of Resources, Environment and Materials, Guangxi University, Nanning 530004, Guangxi, China

[b] School of Electronic Engineering, Guangxi Engineering Research Center for Characteristic Metallic Powder Materials, Guangxi University of Science and Technology, Liuzhou 545006, China

[c] College of Engineering, Mathematics and Physical Sciences, University of Exeter, EX4 4QF, United Kingdom

[d] State Key Laboratory of Materials Processing and Die & Mould Technology, School of Materials Science and Engineering, Huazhong University of Science and Technology, Wuhan, People's Republic of China;

**Corresponding author. E-mail address: D.Chen@st.gxu.edu.cn（Ding Chen）*

**Corresponding author. E-mail address: c_yan@hust.edu.cn（Chunze Yan）*

**Corresponding author. E-mail address: Y.zhu@exeter.ac.uk（Yanqiu Zhu）*

Experimental

Materials

The commercial laser sintering grade PN500W (Polyamide 12, PA12, or Nylon12) powder (D50, 55–65 μm) was supplied by Wanfab®. The commercial laser sintering grade PN500W (Polyamide 12, PA12, or Nylon12) powder (D50, 55–65 μm) was supplied by Wanfab®. The SiC whisker (D500B, 0.1-1 μm, length 5-30 μm, 99%) was supplied by Xuzhou Jiechuang New Material Technology Co. Ltd. $Cu(NO_3)_2 \cdot 3H_2O$ (>98%), benzene-1,3,5-tricarboxylic acid (H_3BTC, >98%), and N, N-dimethylformamide (DMF, >99.8%) were purchased from Alfa Aesar Chemicals. Polyvinylpyrrolidone (PVP, average molecular weight of 1300000) was obtained from Macklin Biochemical Co., Ltd. Methanol (Purity: 99.5%) was purchased from Meyer Chemical Technology Co., Ltd. (Shanghai, China). Ethanol was purchased from Sinopharm Chemical Reagents (Shanghai, China). The water used in the experiments was all deionized water.

Synthesis of PVP-SiC

Firstly, SiC (1 g) was dispersed in 20 ml of ethanol and then sonicated for 1 h. Thereafter, 0.5 g of PVP was added and the mixed solution was stirred (600 rpm) for 2 h at ambient conditions. Centrifugation (8000 rpm, 5 min) was carried out and finally the PVP-SiC product was collected by freeze-drying.

Synthesis of HKUST-1

$Cu_3(BTC)_2$ (HKUST-1) was prepared according to previously reported methods[1]. In general, 10.5 g of $Cu(NO_3)_2$-$3H_2O$ and 5.5 g of H_3BTC (benzene-1,3,5-tricarboxylic acid) were dissolved in 120 ml of mixed solution (DMF: Methanol = 1:1, v/v) and the mixture was sonicated for 20 min to obtain a homogeneous solution. The solution was transferred to a

hydrothermal reactor and kept at 120 °C for 30 hours under static conditions. The solution was washed twice with DMF and ethanol/water solution (1:2, v/v). After centrifugation, the solution was dried in a vacuum oven at 80°C for 24 hours.

Preparation of PVP-SiC-HK

Firstly, silicon carbide (0.5 g) was dispersed in 20 ml of ethanol and then sonicated for 1 h. Thereafter, 0.5 g of PVP was added and magnetically stirred for 2 h (600 rpm) at room temperature. After the stirring was completed, HKUST-1 (0.5 g) was placed in the mixed solution and left to stand for 1h. The product was collected by centrifugation (8000rpm,5min) and freeze-dried.

Characterization

X-ray diffraction (XRD)

The crystal structure investigation was assessed utilizing X-ray diffraction (XRD; Rigaku D/MAX 2500V, Japan) with a step size of 0.03° in the 2θ range of 5-80°.

Fourier transform infrared (FTIR) spectroscopy analysis

Utilizing an FTIR400 spectrometer (PerkinElmer Instrument, US), Fourier transforms infrared (FTIR) spectroscopy was used to characterize the specimens' chemical structure. After being combined with KBr, the samples were formed into tablets. With a 4 cm^{-1} over 16 scans, FTIR spectra in the 4000-400 cm^{-1} wavenumber region were obtained.

Mechanical properties

The mechanical characteristics of the nanocomposites (dumbbell-shaped) were explored by the Mechanics of Materials Experiment System (Model Spec 8801, INSTRON, UK) at a 10 mm/min speed at room temperature. Each material's average was calculated after examining at

least five specimens.

Scanning electron microscopy

Employing a scanning electron microscope (SEM, Sigma 300, ZEISS, Germany) operating at 15 kV, the surface morphology of the phase morphology of PA12 and its nanocomposites was investigated. A small layer of gold was previously sprayed on the samples. Investigating the particles distribution of SiC, P-SiC, HK, and P-SiC-HK powders and PA12 in the matrix required using Energy Disperse Spectroscopy (EDS, Sigma 300, ZEISS, Germany).

Thermal analysis

A 10 °C/min scan rate was operated for the thermogravimetric analysis (TGA, Perkin Elmer-4000, USA) of pure PA12 and its nanocomposites throughout a temperature range of 30-800 °C.

Dynamic differential scanning was applied to measure the nanocomposites' melting and crystallization temperature profiles. Differential scanning calorimetry was carried out with a Mettler instrument calibrated with indium (T, ΔH) and zinc (T). DSC samples of 5-10 mg were weighed in a 40 µl stainless steel pan and computed against an empty pan as reference. The following method was employed for experiments under an 80 ml/min nitrogen flow rate: The samples were heated in DSC from 25 °C to 250 °C with a heating rate of 10 °C·min^{-1}, and then cooled from 250 °C to 25 °C with a heating rate of 10 °C·min^{-1}. Every test was repeated three times. And the STARe package software was operated to investigate melting temperature (Tm), crystallization temperature (T_C), and crystallinity (Xc). The degree of crystallinity Xc of the PA12 phase was computed from DSC curves as follows (Eq. (1)):

$$X_c = \frac{\Delta H\mathrm{m}}{(1 - \emptyset)\Delta H_m^*} \times 100\% \qquad (1)$$

where ϕ is the weight fraction of the dispersed phase in the blends, ΔH_m is the melting enthalpy (J/g) that was calculated from the fusion peak in the DSC curve, and ΔH_m^* is the heat of fusion for completely crystallized PA12 (209.2 J/g).

By a dual cantilever mode and a temperature scan range of 25–350°C, the dynamic mechanical analysis of nanocomposites (DMA, model TA Instruments–Model 850, Newcastle, Delaware, USA) was measured. The energy storage modulus (E'), loss modulus (E"), and loss angle tangent factor (tanδ) were evaluated as functions of temperature at a heating rate of 3°C/min.

Thermal conductivity

The thermal conductivity of all powder samples was measured using the Hot Disk TPS-2500 thermal constants analyzer at room temperature, following ISO 22007-2 standards. The powder samples were slightly compressed into discs, and each was tested in duplicate at 30°C to ensure accuracy in the results.

Flame test

According to ISO 5660 standards, a flame test was conducted on a cone calorimeter (Fire Testing Technology, UK) using 100 × 100 × 3 mm^3 specimens. A horizontal external heat flux of 35 kW/m^2 was applied to each specimen. Three tests were performed on all samples.

Raman spectroscopy

A 514.5 nm argon laser line was utilized as the excitation source for the laser Raman spectroscopy (LRS) experiments using a SPEX-1403 laser Raman spectrometer (SPEX Co., United States) under room temperature.

XPS analysis

To use a VG ESCALB MK-II Electron Spectrometer (Al K excitation source at 1486.6 eV), X-ray photoelectron spectroscopy (XPS) was conducted on the samples to confirm the elemental composition of SiC, P-SiC, HK, and P-SiC-HK nanoparticles in the PA12 nanocomposites chars and hybrids.

Thermogravimetric analysis–infrared spectrometry analysis

Thermogravimetric analysis–infrared spectrometry (TG–IR) was performed using a TGA4000 thermogravimetric analyzer connected to an IR400 FTIR spectrophotometer(Perkin Elmer, USA). The samples were put in an alumina crucible and heated from 25 to 800 °C. The heating rate was 20 °C/min (nitrogen atmosphere, flow rate of 40 ml/min).

Pyrolysis-gas chromatography/mass spectrometry (PY-GC–MS) analysis

Pyrolysis-gas chromatography/mass spectrometry (PY-GC–MS) was performed on a TG-GC-MS system (Perkin Elmer, USA). The pure PA12 and its nanocomposites were heated to 800 °C at a heating rate of 20°C/min. The data of mass spectra were examined by the NIST library.

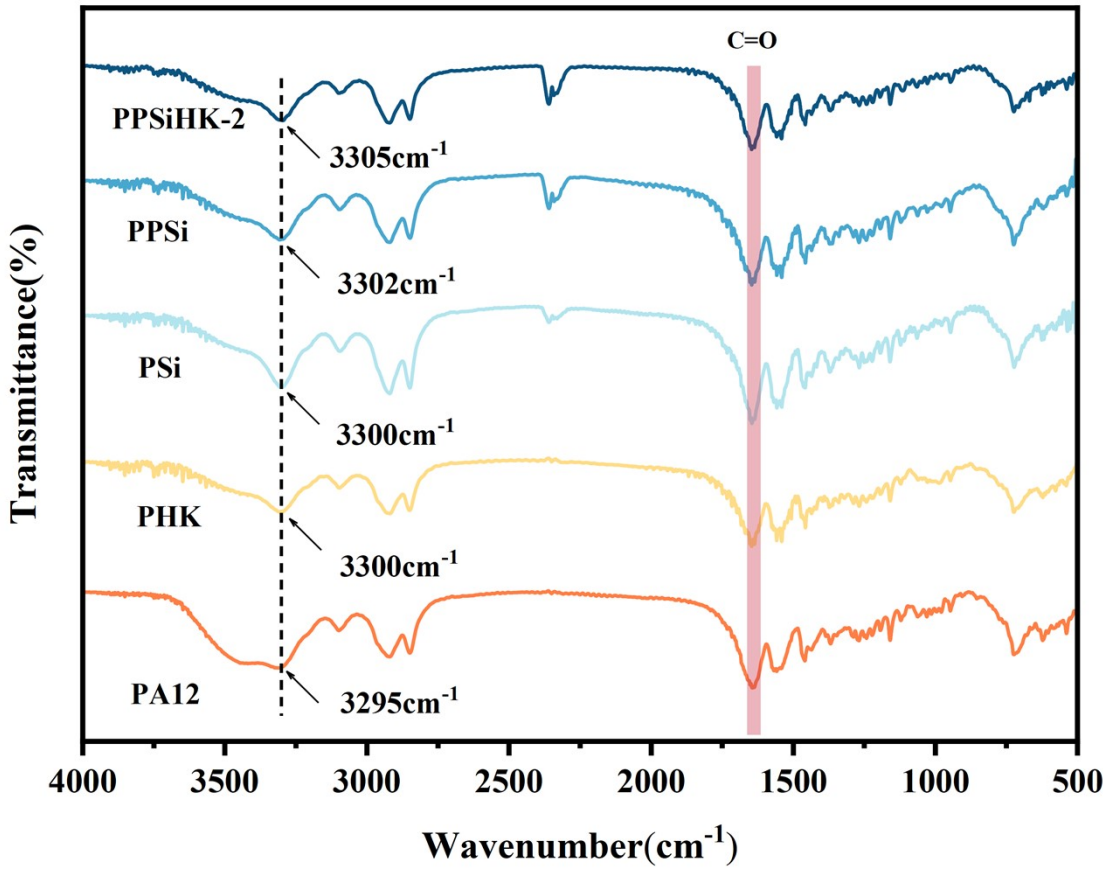

Figure S1. FT-IR spectra of pure PA12 and its composites.

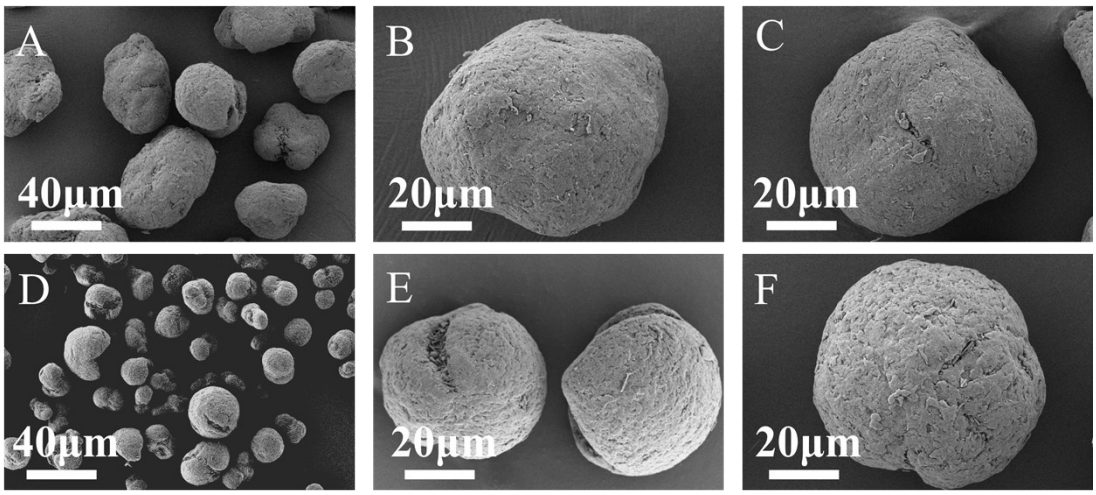

Figure S2. SEM images of powders: (A~C) PA12; (D~F) PPSiHK-2.

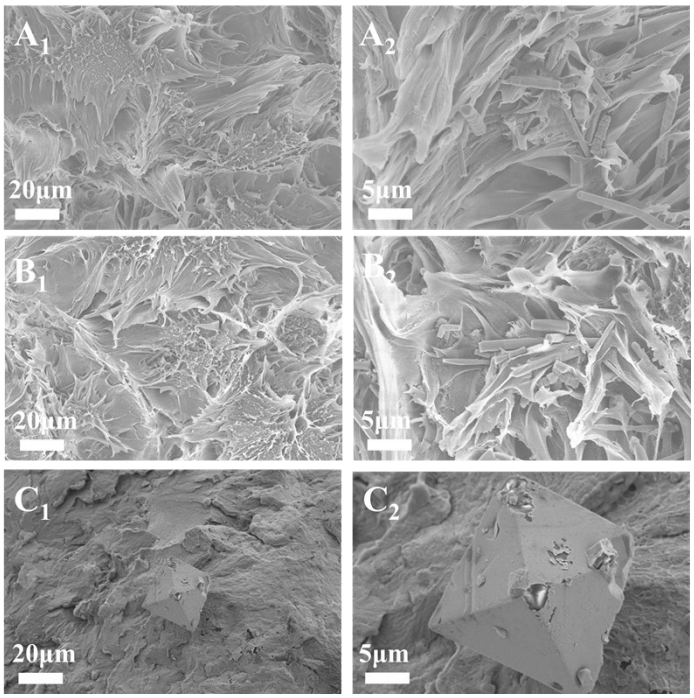

Figure S3. SEM images of the fracture surface of PSi, PPSi, and PHK nanocomposites: (A_1, A_2) PSi; (B_1, B_2) PPSi; (C_1, C_2) PHK.

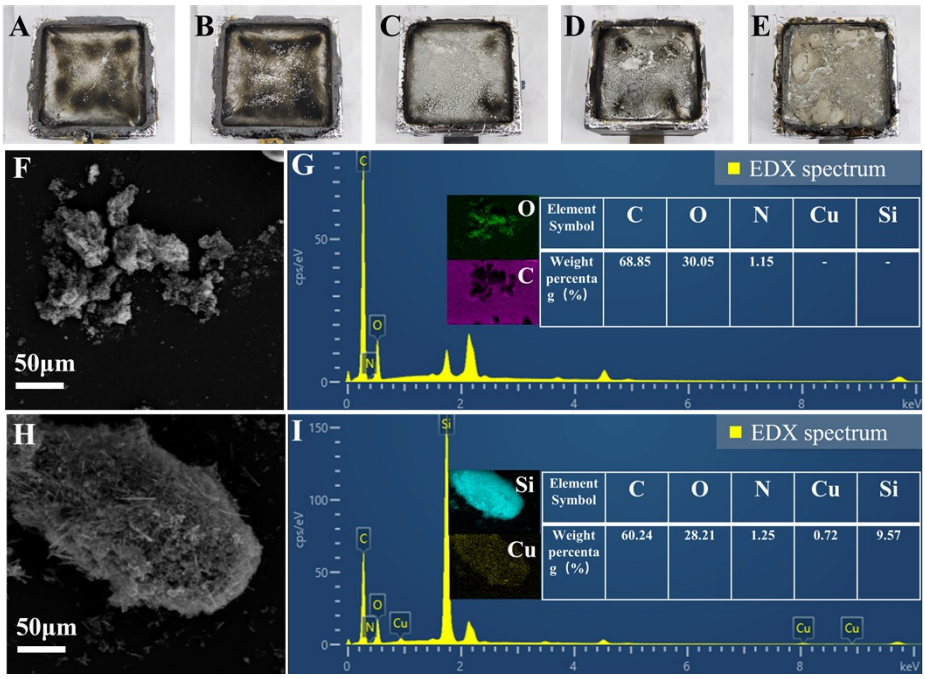

Figure S4. Digital photographs of char residue of (A) pure PA12, (B) PSi, (C) PPSi, (D) PHK and (E) PPSiHK-2 nanocomposite. EDS energy analysis of char residue: (F) pure PA12 and its surface element composition (G); (H) PPSiHK-2 and its surface element composition (I).

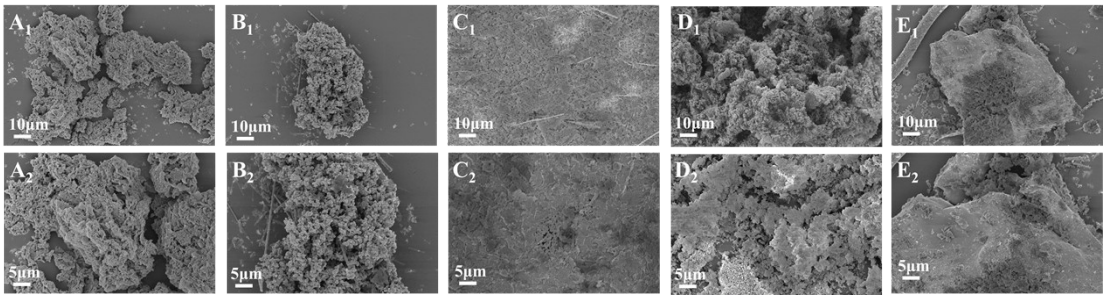

Figure S5. SEM images of char residues of (A_1, A_2) pure PA12; (B_1, B_2) PSi; (C_1, C_2) PPSi; (D_1, D_2) PHK; (E_1, E_2) PPSiHK-2.

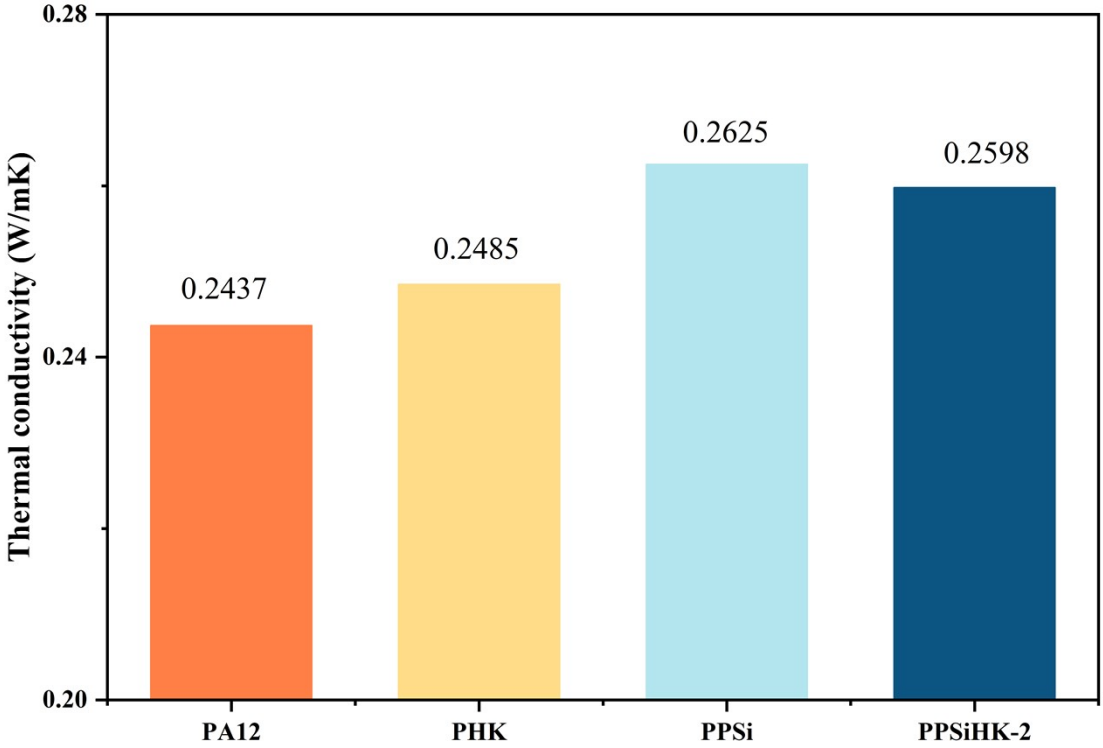

Figure S6. Thermal conductivity of powders: PA12, PHK, PPSi and PPSiHK-2.

Table S1. DSC data of pure PA12, PSi, PPSi, PHK, and PPSiHK-X (X=0.5, 1, 2, 4) powders. T_m is the melting temperature; $T_{m\text{-onset}}$ is the onset melting temperature; T_C is the crystallization temperature; $T_{c\text{-onset}}$ is the onset crystallization temperature; T_W is the sintering window temperature.

Sample Name	$T_{m\text{-}onset}$ (°C)	T_m(°C)	$T_{c\text{-}onset}$	T_C(°C)	T_W(°C)
PA12	173.41	180.07	155.4	151.39	18.01
PSi	176.17	182.2	187.51	157.83	18.34
PPSi	177.06	182.8	185.92	157.24	19.82
PHK	176.2	182.2	156	153.4	20.15
PPSiHK-0.5	174.67	181.06	156.16	152.28	18.51
PPSiHK-1	175.5	181.7	154.7	151.9	20.8
PPSiHK-2	176.28	181.38	184.99	153.26	23.02
PPSiHK-4	176.01	181.61	185.22	154.19	21.82

Table S2. TGA data of pure PA12, PSi, PPSi, PHK, and PPSiHK-X (X=0.5, 1, 2, 4) nanocomposites fabricated by SLS in the N_2 atmosphere. T_{onset} represents the onset temperature of deterioration. T_p is the maximum weight loss rate temperature.

Sample	T_{onset}(°C)	T_P (°C)	Char Residue at 700 °C (wt%)
PA12	425.57	481	1.5
PSi	429.41	478.75	3.036
PPSi	426.3	477.02	2.945
PHK	430.37	476.86	1.90
PPSiHK-0.5	426.31	479.5	1.894
PPSiHK-1	431.86	474.71	2.722
PPSiHK-2	434.96	482.47	2.206
PPSiHK-4	425.83	478.85	3.239

Table S3. DMA data of pure PA12, PSi, PPSi, PHK, and PPSiHK-X (X=0.5, 1, 2, 4) nanocomposites fabricated by SLS.

Sample	E′ (MPa)	Tg of PA12(°C)
PA12	944.95	60.23
PSi	963.08	58.34
PPSi	980.582	60.97
PHK	1156.12	57.06
PPSiHK-0.5	1099.01	61.05
PPSiHK-1	1162.7	58.63
PPSiHK-2	1211.58	60.85
PPSiHK-4	1076.99	56.74

Table S4. Flame test of pure PA12, PSi, PPSi, PHK, and PPSiHK-2 nanocomposites fabricated by SLS.

Sample	TTI	pHRR (kW/m^2)	THR (MJ/m^2)	pSPR (m^2/s)	TSP(m^2)	AEHC(MJ /KG)
PA12	79s	892.330	155.444	0.0383	4.994	32.756
PSi	62s	798.011	148.713	0.0364	5.632	28.884
PHK	39s	789.611	137.400	0.0364	5.342	34.703
PPSi	50s	859.693	152.240	0.0374	6.021	28.579
PPSiHK-2	59s	779.262	145.275	0.0337	6.106	25.730

Table S5. The state of flame retardancy performance of polymer composites based on PA12 containing different additives in terms of the FRI as a function of weight percent (wt.%).

samples	wt.%	pHRR(Kw/m^2)	THR(MJ/m^2)	Ref
PA12	-	775.5 ± 13	38.9 ± 0.8 kJ/g	[2]
LDH@GF-20	10	760.9 ± 17	34.8 ± 1.3 kJ/g	[2]
PA12	-	1635	115.8	[3]
POSS	3	1521	112.4	[3]

PA12	-	1580	151	[4]
Exolit OP950	30	783	138	[4]
Aflammit PCO900	30	1224	145	[4]
PA12	-	935.682	159.911	[5]
IF-WS_2	2	848.132	177.699	[5]
PA2200(PA12)	-	1244±150	139 ± 4	[6]
Nipol 1411 rubber	20	920±80	132±9	[6]
Zealloy 1422A rubber	20	1013±115	124±4	[6]
PA12	-	892.330	155.444	**This work**
PVP-SiC-HK	2	779.262	145.275	**This work**

152

153

Reference

[1] Q.V. Thi, N.Q. Nguyen, I. Oh, J. Hong, C.M. Koo, N.T. Tung, D. Sohn, Thorny trunk-like structure of reduced graphene oxide/HKUST-1 MOF for enhanced EMI shielding capability, Ceramics International 47(7) (2021) 10027-10034. https://doi.org/10.1016/j.ceramint.2020.12.149.

[2] B. Lecouvet, M. Sclavons, S. Bourbigot, C.J.P.f.a.t. Bailly, Towards scalable production of polyamide 12/halloysite nanocomposites via water-assisted extrusion: mechanical modeling, thermal and fire properties, Polymers for advanced technologies 25(2) (2014) 137-151.

[3] S. Gentiluomo, A.D. Veca, M. Monti, M. Zaccone, M.J.P.D. Zanetti, Stability, Fire behavior of polyamide 12 nanocomposites containing POSS and CNT, Polymer Degradation and Stability 134 (2016) 151-156.

[4] M. Batistella, A. Regazzi, M.F. Pucci, J.-M. Lopez-Cuesta, O. Kadri, D. Bordeaux, F. Ayme, Selective laser sintering of polyamide 12/flame retardant compositions, Polymer Degradation and Stability 181 (2020) 109318. https://doi.org/https://doi.org/10.1016/j.polymdegradstab.2020.109318.

[5] D. Chen, X. Qin, X. Cao, N. Wang, Y. Zhu, Selective laser sintering of PEG treated inorganic fullerene-like tungsten disulfide nanoparticles/polyamide 12 nanocomposites and fire safety behavior, Chemical Engineering Journal 450 (2022) 137644. https://doi.org/https://doi.org/10.1016/j.cej.2022.137644.

[6] M. Batistella, M.F. Pucci, A. Regazzi, J.-M. Lopez-Cuesta, O. Kadri, D. Bordeaux, F. Ayme, Fire Behavior of Polyamide 12/Rubber Formulations Made by Laser Sintering, Materials, 15.5 2022.